

Study on Emergency Braking Control Strategy Considering Road Surface Friction Coefficient

Jiashun Feng

Tianjin University of Science and Technology, Tianjin 300222, China

Abstract: *This study systematically demonstrated, through simulation validation, the effectiveness and safety of the proposed strategy across the entire road surface perception-decision-execution chain. It enables real-time acquisition of road surface friction coefficients and formulates an emergency braking control strategy, providing a reliable technical foundation for the engineering application of intelligent braking systems (AEB). The research outcomes not only meet international safety standards such as E-NCAP but also offer critical practical insights for optimizing active safety algorithms in future intelligent connected vehicles.*

Keywords: Intelligent Vehicle, Automatic Emergency Braking (AEB) Strategy, Staged Braking, Road Surface Friction Coefficient Estimation.

1. Introduction

With the sustained growth of the national economy, the widespread adoption of automobiles has significantly improved transportation accessibility and enhanced the quality of life for the general population. Statistical data indicate that global automobile sales surged to 95.6 million units in 2018. However, according to the latest report released by the United Nations, road traffic accidents annually result in approximately 1.25 million fatalities and 50 million non-fatal injuries, with associated economic losses amounting to \$1.85 trillion USD [1]. Traffic safety research demonstrates that approximately 90% of road accidents are attributable to drivers' errors in judgment or improper vehicle handling [2]. Severe rear-end collisions are primarily attributable to insufficient braking force or delayed brake response from the following vehicle [3]. To effectively mitigate these risks, Autonomous Emergency Braking (AEB) systems have demonstrated significant effectiveness through real-time risk assessment and intelligent braking decision-making: equipped vehicles exhibit an overall 38% reduction in rear-end collision rates compared to non-equipped vehicles [4]. It should be emphasized that dynamic variations in tire-road adhesion conditions directly affect the maximum achievable deceleration of vehicles, thereby significantly constraining the adaptability of AEB control strategies. Current research predominantly maintains maximum braking deceleration as a fixed parameter, resulting in insufficient braking performance or delayed response on low-adhesion surfaces, while inducing over-aggressive braking or premature activation on high-adhesion surfaces. Consequently, real-time accurate identification of tire-road adhesion coefficients has emerged as a critical component for enhancing braking accuracy and environmental adaptability of AEB systems. The time-varying characteristics of road adhesion properties determine the maximum achievable deceleration range of vehicles, exerting a significant influence on AEB control strategies. Existing studies continue to treat vehicle maximum braking deceleration as a constant parameter [5-6]. Building upon the aforementioned research foundation, this study develops an online tire-road adhesion state identification method based on vehicle dynamic response characteristics, which significantly enhances environmental adaptability to time-varying road conditions while maintaining economic feasibility. Additionally, a multi-level AEB decision-making

architecture is proposed through systematic risk assessment of dynamic traffic participants, enabling precise determination of braking activation timing. This approach optimizes braking smoothness and occupant comfort while ensuring traffic safety. Furthermore, synergistic integration of the adhesion state identification module with hierarchical control logic systematically enhances the robustness and response accuracy of AEB systems across varying adhesion surfaces, establishing a technical foundation for effectively mitigating rear-end collisions and other traffic accidents [7].

2. Methodology

2.1 Development of Vehicle Dynamics Models

Along with the movement of the target, the sink node timely notifies the sensor nodes in the relevant detection area to join in the process of target tracking. Figure 1 is the flow chart of the moving target tracking process. The tire-road adhesion coefficient represents a critical physical parameter in vehicle dynamics control systems, where its identification accuracy directly influences driving stability and active safety performance under emergency braking conditions. Therefore, achieving high-reliability online identification of this parameter holds significant engineering importance. This section embeds the Dugoff tire mechanics model into a vehicle dynamics modeling framework and constructs an adaptive estimation algorithm based on Kalman filter theory to enable dynamic tracking and real-time identification of the tire-road adhesion coefficient.

Considering the highly nonlinear characteristics and multivariable strong coupling dynamics of vehicle systems, combined with susceptibility to external disturbances such as road excitations and wind loads during actual operation, establishing a mathematical model that both accurately characterizes system dynamics and maintains engineering practicality becomes a prerequisite for subsequent control strategy design and validation. While preserving essential vehicle motion characteristics, this study implements reasonable simplifications and necessary constraints in the dynamics model, and establishes the following fundamental assumptions. As shown in Figure 1:

(1) Neglect the effects of tire aligning torque;

- (2) Assume rigid suspension without considering coupling interactions between suspension and tires;
- (3) Ignore lateral load transfer caused by steering or other factors;
- (4) Assume planar motion parallel to the ground surface.

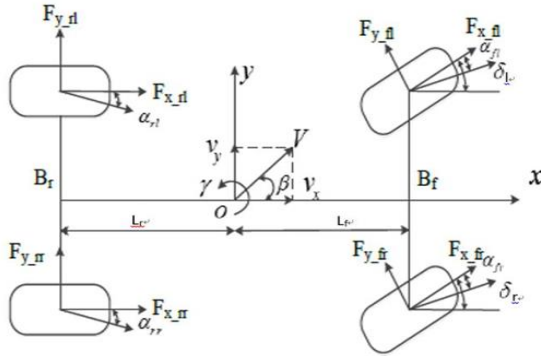


Figure 1: Seven-Degree-of-Freedom Vehicle Dynamics Model

To accurately characterize vehicle dynamic behavior, this study employs a body-fixed coordinate system with its origin O located at the vehicle centroid. In the reference

$$I_z \dot{\omega}_z = \frac{B_f}{2} (F_{xfr} \cos \delta_r - F_{xfl} \cos \delta_l - F_{yfr} \sin \delta_r + F_{yfl} \sin \delta_l) + \frac{B_r}{2} (F_{xrr} - F_{xrl}) + L_f (F_{xfl} \sin \delta_l + F_{yfl} \cos \delta_l + F_{xfr} \sin \delta_r + F_{yfr} \cos \delta_r) - L_r (F_{yrl} + F_{yrr}) \quad (3)$$

Longitudinal Forces of Individual Tires:

$$F_{Zfl} = m_w g + \frac{m_b g L_r}{2L} - \frac{m_b h g a_x}{2L} - \frac{m_b h g a_y}{2B_f} \quad (4)$$

$$F_{Zfr} = m_w g + \frac{m_b g L_r}{2L} - \frac{m_b h g a_x}{2L} + \frac{m_b h g a_y}{2B_f} \quad (5)$$

$$F_{Zrl} = m_w g + \frac{m_b g L_f}{2L} + \frac{m_b h g a_x}{2L} - \frac{m_b h g a_y}{2B_r} \quad (6)$$

$$F_{Zrr} = m_w g + \frac{m_b g L_f}{2L} + \frac{m_b h g a_x}{2L} + \frac{m_b h g a_y}{2B_r} \quad (7)$$

m : vehicle mass; B_f : front track width; B_r : rear track width; L_f : rear wheelbase;

2.2 Development of the Dugoff Tire Model

Development of a high-fidelity tire model with superior curve-fitting accuracy enables precise characterization of vehicle dynamic behavior during operation. Such models provide reliable feedback parameters for vehicle control systems, allowing precise execution commands to fully exploit the vehicle's performance potential. Additionally, as the critical interface between the vehicle and the road surface, tire-road interactions facilitate effective estimation of key road parameters such as adhesion coefficients and surface roughness.

The integration of the Dugoff tire model establishes a foundational physical framework for adhesion coefficient estimation algorithms. Its core contribution lies in the explicit mechanical mapping relationship between tire longitudinal/lateral forces and road adhesion characteristics. Through normalization factor-based dimensionless processing of tire forces, this model enhances the physical

configuration where the vehicle remains stationary on a horizontal road surface, the X-axis aligns longitudinally along the vehicle's forward direction, the Y-axis extends laterally to the left (orthogonal to the X-axis), and the Z-axis points vertically upward, with all three axes mutually orthogonal. Based on this coordinate framework, vehicle attitude motion can be decomposed into three critical rotational degrees of freedom: roll rotation about the X-axis, pitch rotation about the Y-axis, and yaw rotation about the Z-axis. This coordinate system establishes a unified geometric reference for quantitative characterization of vehicle motion states and dynamics modeling. The longitudinal motion differential equation of the vehicle is expressed as:

$$m(\dot{v}_x - v_y \omega_z) = F_{xfl} \cos \delta_l + F_{xfr} \cos \delta_r - F_{yfl} \sin \delta_l - F_{yfr} \sin \delta_r + F_{xrl} + F_{xrr} \quad (1)$$

Vehicle Lateral Motion Differential Equation:

$$m(\dot{v}_y + v_x \omega_z) = F_{xfl} \sin \delta_l + F_{xfr} \sin \delta_r + F_{yfl} \cos \delta_l + F_{yfr} \cos \delta_r + F_{yrl} + F_{yrr} \quad (2)$$

Vehicle Yaw Motion Differential Equation:

interpretability of estimation algorithms while effectively capturing the nonlinear mechanical behavior under varying slip conditions. Without such physically grounded tire models, adhesion coefficient estimation would degrade to theoretical-unjustified data-driven fitting processes, failing to meet the dual requirements of precision and real-time performance in engineering applications. During modeling, simplifying assumptions are adopted: the tire-road interaction is equivalent to pure sliding friction mechanisms. Based on this premise, analytical expressions for tire longitudinal and lateral forces are derived as follows. As shown in Figure 2:

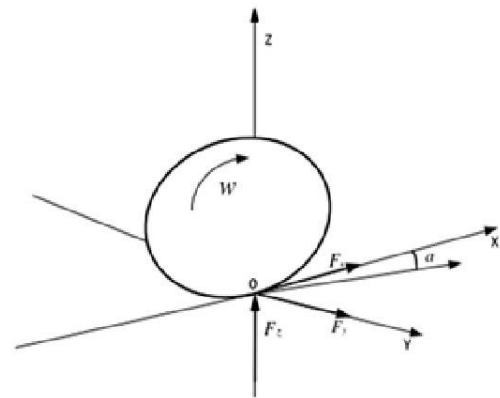


Figure 2: Force Analysis Schematic of the Dugoff Tire Model

2.3 Basic Technology of Moving Target Tracking in Wireless Sensor Networks

An adhesion coefficient estimation algorithm based on the Unscented Kalman Filter (UKF) is proposed, where the implementation workflow involves the following steps: Initially, sensor data including front wheel steering angle,

longitudinal/lateral accelerations, and outputs from the vehicle dynamics model are integrated and fed into the UKF-based vehicle state estimator. This module dynamically computes critical vehicle states required for adhesion coefficient estimation, such as longitudinal/lateral velocities and yaw rate. Subsequently, the estimated states are combined with the Dugoff tire model to generate normalized longitudinal and lateral tire forces through dimensionless processing via a normalization factor. Finally, the normalized tire forces, alongside sensor-measured parameters (e.g., front wheel steering angle) and UKF-estimated vehicle states, are input into the road adhesion coefficient estimator to achieve real-time and precise quantification of the road adhesion coefficient. This framework establishes a closed-loop estimation system where the interplay between vehicle

dynamics, tire-road interaction modeling, and Kalman filtering ensures both physical interpretability and engineering feasibility. As shown in Figure 3.

To rigorously validate the effectiveness of the UKF-based estimation algorithm, simulation validations are conducted under three distinct road adhesion scenarios: low-adhesion coefficient surfaces ($\mu=0.3$), high-adhesion coefficient surfaces, and split-friction road conditions (asymmetric μ distribution between left and right wheels). The estimation performance is evaluated by comparing the estimated adhesion coefficients against actual road adhesion values, thereby assessing the estimator's design validity. The simulation employs the E-Class vehicle model from CarSim, with key vehicle parameters listed in Figure 4.

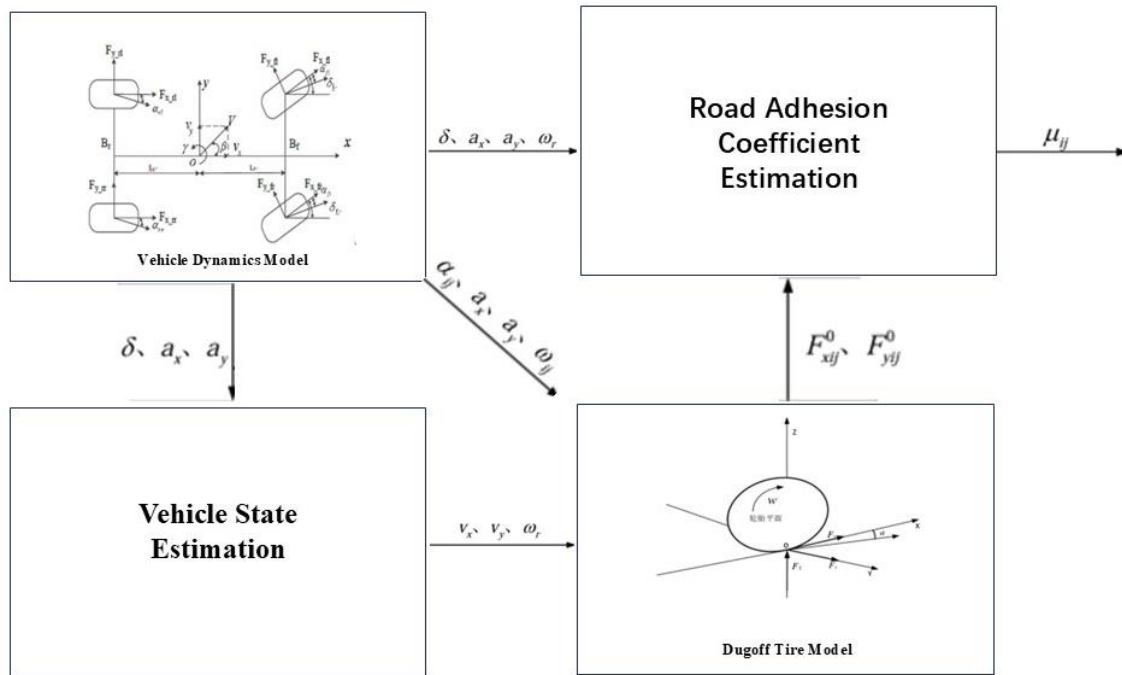


Figure 3: Road Surface Friction Coefficient Estimation Flowchart

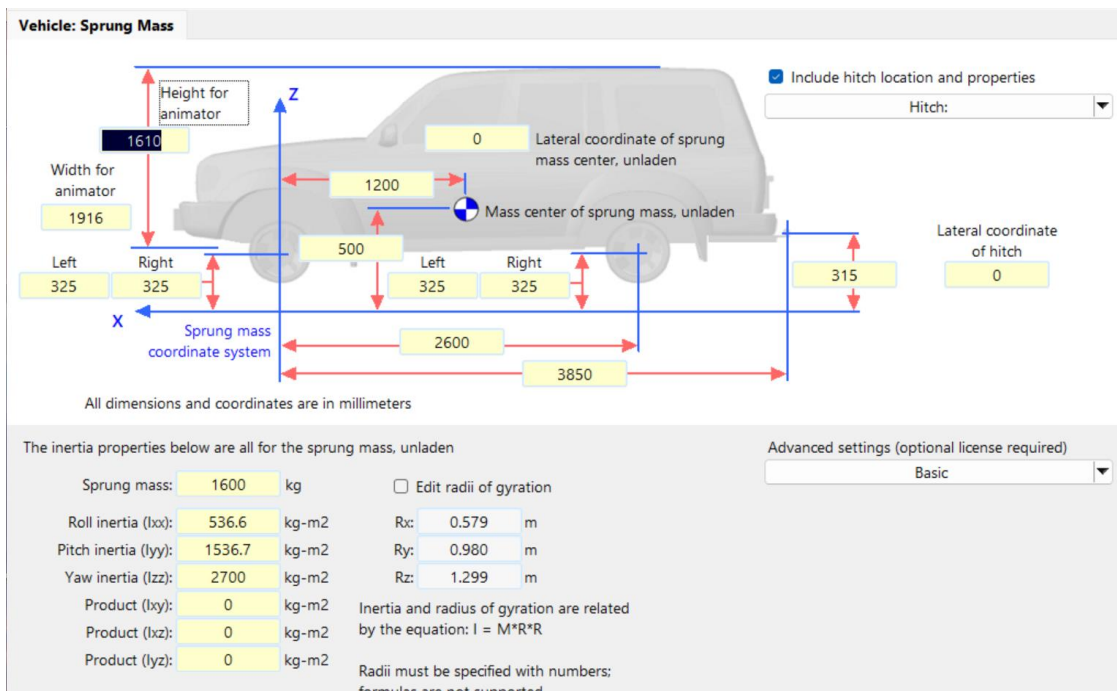


Figure 4: Carsim Vehicle Parameters Configuration Interface

Three distinct roadway scenarios with high-adhesion ($\mu=0.8$), low-adhesion ($\mu=0.3$), and stepwise friction transition adhesion coefficients are established for simulation testing. The road setup interface in CarSim, as illustrated in Figure 5-6, demonstrates the implementation of these test conditions.

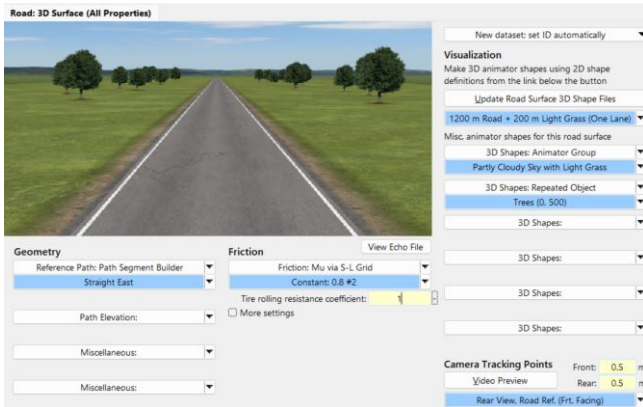


Figure 5: Carsim Road Parameters Configuration Interface

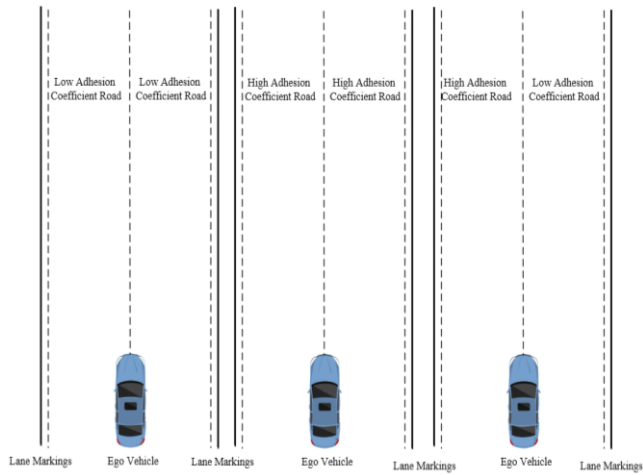


Figure 6: Road Parameters Configuration Schematic

The simulation is conducted on a flat straight road surface with a road adhesion coefficient set to 0.3 and an initial vehicle speed of 20 km/h. The low-adhesion coefficient estimation results are illustrated in the Figure 7.

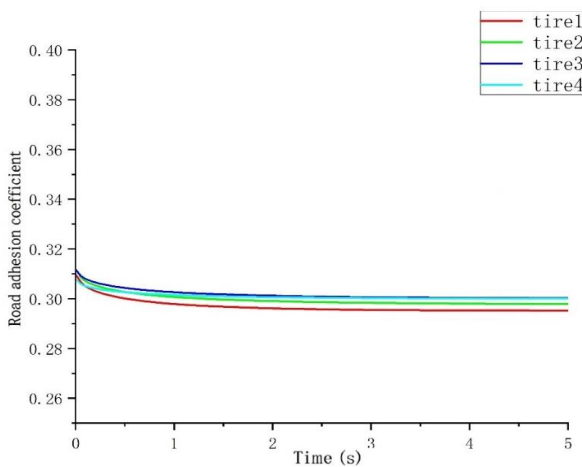


Figure 7: Simulation Results on Low Road Surface Friction Coefficient Road

The simulation is conducted on a flat straight road surface with a road adhesion coefficient set to 0.8 and an initial vehicle speed of 20 km/h. The low-adhesion coefficient estimation results are illustrated in the Figure 8.

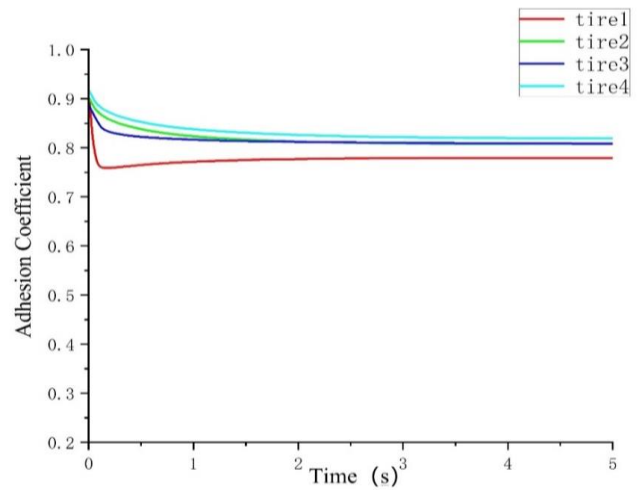


Figure 8: Simulation Results on High Road Surface Friction Coefficient Road

The simulation is configured on a flat straight road surface with asymmetric adhesion distribution: left-side adhesion coefficient set to 0.8 and right-side adhesion coefficient set to 0.3. The vehicle is initialized at a speed of 20 km/h, and the low-adhesion coefficient estimation results are illustrated in Figure 9.

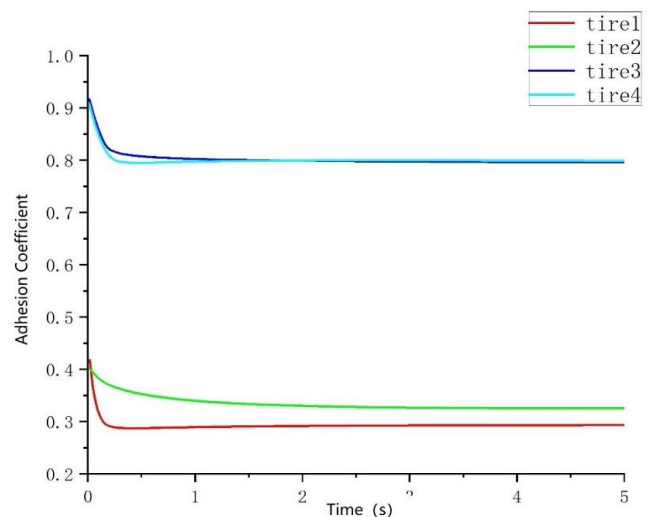


Figure 9: Simulation Results on Split Road Surface Friction Coefficient Road

The simulation results demonstrate that the UKF-based estimation algorithm achieves a convergence time of approximately 0.15 seconds for the first response and 0.18 seconds for the second response under low-adhesion conditions ($\mu=0.3$). Under asymmetric adhesion conditions (left-side $\mu=0.8$, right-side $\mu=0.3$), the algorithm exhibits a convergence time of approximately 0.21 seconds to stabilize near the true adhesion coefficient value.

2.4 AEB Hierarchical Control Strategy Based on Road Adhesion Coefficient Estimation

As illustrated in the figure eleven, the Autonomous Emergency Braking (AEB) strategy comprises three functional modules: Environmental Perception, High-Level Control, and Low-Level Control. Prior to detailed component analysis, this study establishes the overall system architecture design to ensure seamless integration of these modules within the AEB framework. As shown in Figure 10.

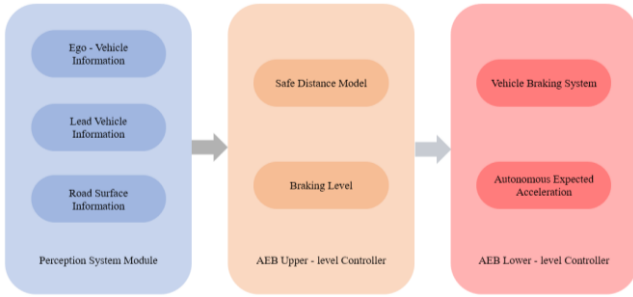


Figure 10: Overall System Architecture Design Diagram

To realize closed-loop control functionality in the Autonomous Emergency Braking (AEB) system, the environmental perception module first performs real-time fusion of multi-sensor data, including the preceding vehicle's position and dynamic states (stationary, constant-speed, or decelerating), road adhesion coefficient, and ego-vehicle dynamics parameters. The high-level decision module generates three-tier intervention thresholds—collision warning threshold, staged braking activation threshold, and emergency braking activation threshold—through a dynamic safety distance model that integrates road adhesion conditions and relative kinematic features (relative distance, relative velocity). These thresholds enable differentiated braking commands to be output dynamically.

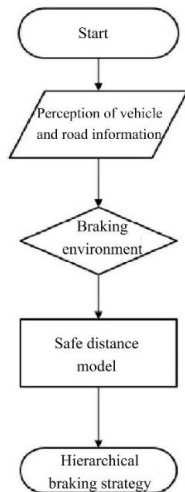


Figure 11: AEB Staged Strategy Architecture

The AEB system employs three thresholds S_w , S_d , and S_b to define a hierarchical braking protocol: in standby mode, no intervention occurs when obstacles are undetected or relative distances remain safe; when the distance reduces to S_w , audible/visual alerts prompt driver action; transitions to S_d activate smooth automated deceleration for comfort; and culminating at S_b , full-force braking engages with optimal deceleration to minimize stopping distance. This strategy dynamically integrates real-time relative motion and road

adhesion data, enabling seamless phase transitions while enhancing hazard response reliability, suppressing false triggers, and optimizing ride comfort. As shown in Figure 11.

The braking process in the Autonomous Emergency Braking (AEB) system is categorized into two distinct stages: moderate braking and full-force braking. The achievable deceleration levels for both stages are determined by road adhesion conditions and are visually represented in the subsequent figure thirteen. The vehicle braking process is further subdivided into four sequential phases, ensuring adaptive control logic across dynamic driving scenarios. As shown in Figure 12.

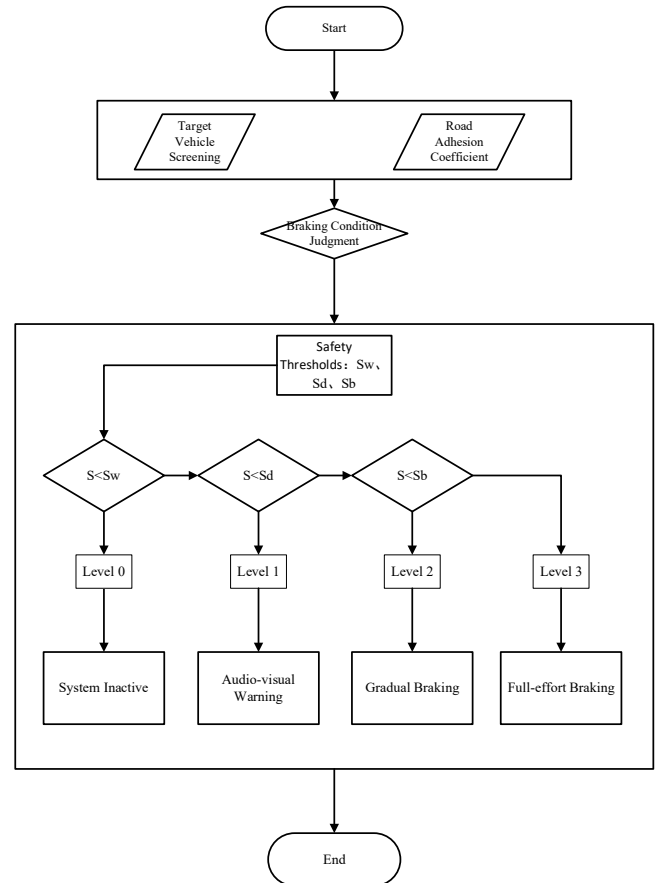


Figure 12: AEB Staged Braking Strategy

2.5 Simulation-Based Validation

This study is conducted based on the technical specifications of E-NCAP and C-NCAP test protocols. A dry asphalt pavement surface with standard tire configurations and specified tire pressure levels was employed, with the road surface friction coefficient established at 0.85. An extreme test scenario was developed, and the parameter configurations for each test scenario are presented in the following Table 1.

Table 1: AEB Staged Braking Operating Conditions

Number	Test scenarios	host vehicle speed (km/h)	leading vehicle speed (km/h)	braking deceleration of leading vehicle (m/s ²)	initial distance (m)
1	Car-to-Car Rear-end Moving (CCRM)	50	40	-6	50

3. Results and Discussion

3.1 Simulation Test Results and Analysis

According to E-NCAP specifications for the leading vehicle deceleration test scenario, the host vehicle and leading vehicle speeds are set to 50 m/s and 40 m/s respectively, with an initial separation distance of 50 m and a leading vehicle

braking deceleration of 6 m/s^2 . Simulation results are shown in the Figure13-15.

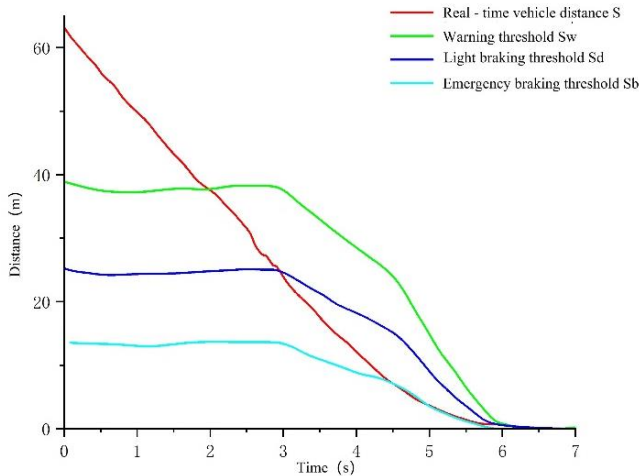


Figure 13: Real-Time Inter-Vehicle Distance and Safety Distance Threshold

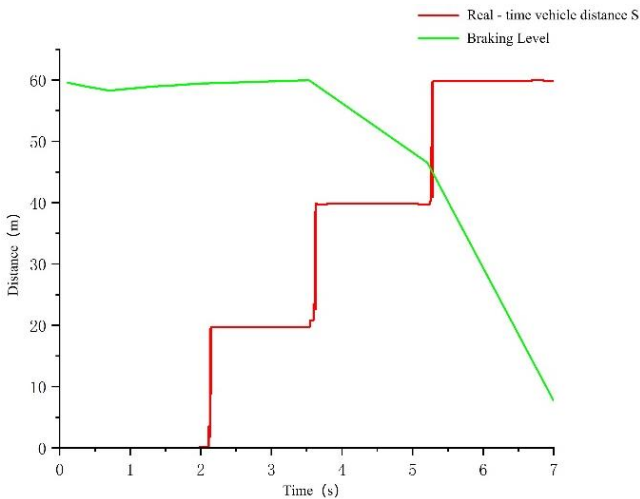


Figure 14: Warning Level and Host Vehicle Speed

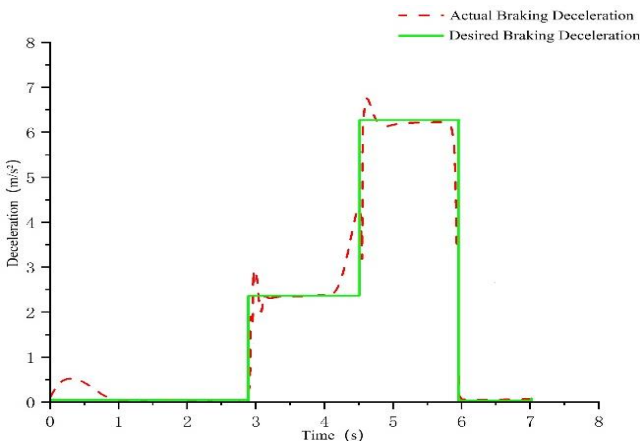


Figure 15: Desired and Actual Deceleration Profiles

During the host vehicle's forward motion, the real-time distance between the two vehicles sequentially reaches the auditory warning threshold, the moderate braking distance, and the emergency braking threshold. Upon receiving hierarchical safety signals at different levels, the system subsequently initiates deceleration and stop maneuvers for the host vehicle. The figure illustrates the desired and actual deceleration profiles during braking, demonstrating that the deceleration follows the desired trajectory. Simulation results

confirm that the Automatic Emergency Braking (AEB) system generates accurate braking commands under this test condition, ensuring braking safety.

In the simulation process, the road surface friction coefficient was set to 0.6, representing wet asphalt conditions. The initial distance between the host vehicle and the leading vehicle was set to 50 m, with the host vehicle operating at a speed of 45 km/h while the leading vehicle remained stationary. Each test condition was divided into two simulations: the first simulation implemented a road surface recognition-based Automatic Emergency Braking (AEB) strategy, while the second simulation utilized a conventional AEB strategy without road surface recognition. The primary focus is to compare the inter-vehicle distance and warning trigger timing between the two simulations. As shown in Figure 16-17.

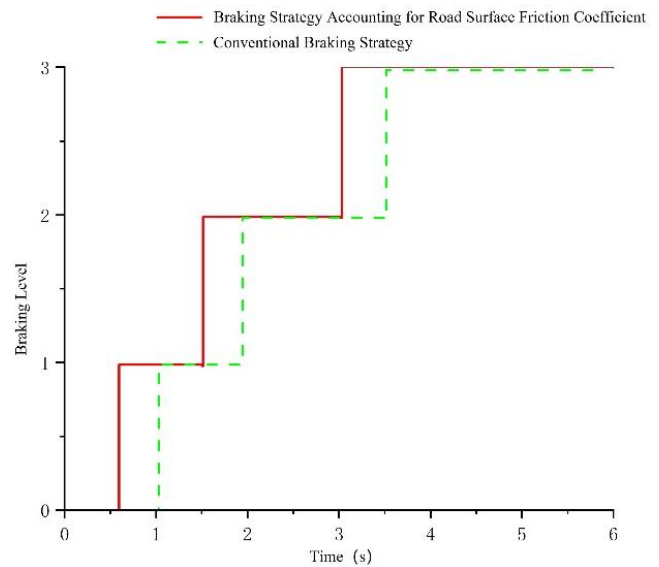


Figure 16: Warning Experiment Comparison

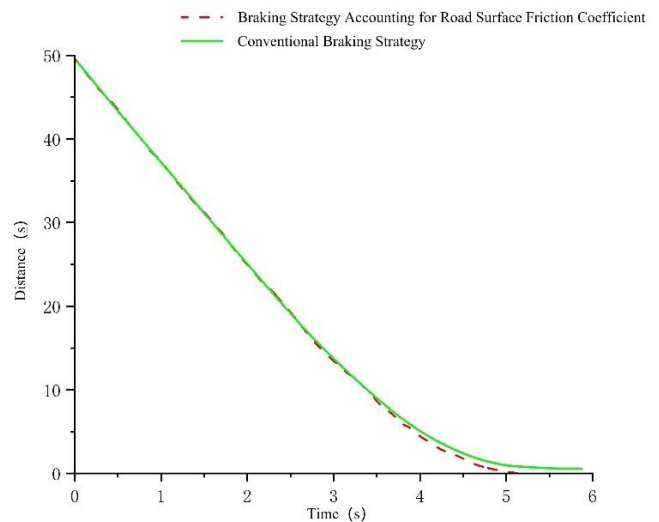


Figure 17: Inter-Vehicle Distance Comparison

Figures 16 and 17 present the simulation results of relative safety distance and collision warning performance under two Automatic Emergency Braking (AEB) strategies. As shown in Figure 18, the road surface condition-aware warning strategy successfully avoids collision, achieving a minimum separation distance of approximately 0.7 m between the vehicles. In contrast, the conventional AEB strategy results in a collision. This demonstrates that the proposed strategy

enhances vehicle driving safety.

4. Conclusion

Automatic Emergency Braking (AEB) is a critical component of vehicle active safety systems. To address variations in road surface friction coefficients, this study proposes an AEB control strategy based on friction coefficient estimation for vehicle AEB systems. By utilizing the Carsim-Simulink co-simulation platform, AEB test scenarios under varied road surface conditions were established and compared with conventional single-stage braking AEB strategies based on fixed trigger thresholds. Simulation results demonstrate that the proposed AEB strategy, while maintaining safety performance, achieves lower braking jerk and improves ride comfort compared to traditional single-stage braking approaches.

Acknowledgments

We sincerely thank our fellow students for their insightful discussions, constructive suggestions, and unwavering support throughout this research.

References

- [1] Q. Zhang et al. (2016). Human factors analysis of road traffic accidents in China. *Automobile Applied Technology*, no.6, p.7-8, 27.
- [2] P. Raj and G. C. Deka (2018). *Blockchain technology: platforms, tools and use cases*. Academic Press, vol.11, p.1-278.
- [3] X. Xiang et al. (2014). Research on a DSRC-based rear-end collision warning model. *IEEE Transactions on Intelligent Transportation Systems*, vol.15, no.3, p.1054-1065.
- [4] B. Fildes et al. (2015). Effectiveness of low speed autonomous emergency braking in real-world rear-end crashes. *Accident Analysis and Prevention*, vol.81, p.24-29.
- [5] D. Y. Feng et al. (2016). Key parameter optimization method for AEB systems in rear-end collision avoidance. *Automotive Technology*, no.11, p.8-12.
- [6] B. Zhu et al. (2016). Vehicle longitudinal collision warning strategy based on road adhesion coefficient estimation. *Automotive Engineering*, vol.38, no.4, p.446-452.
- [7] Y. Z. Ma et al. (2019). System algorithm for AEB in commercial vehicles on curved roads. *Journal of Jiangsu University (Natural Science Edition)*, vol.40, no.4, p.386-390.